JOURNAL OF CATALYSIS **122,** 415–428 (1990)

Generation of Gaseous Radicals by a V–Mg–O Catalyst during Oxidative Dehydrogenation of Propane

KIMMAI T. NGUYEN AND HAROLD H. KUNG[1]

Ipatieff Laboratory and Department of Chemical Engineering, Northwestern University,
Evanston, Illinois 60208

Received July 26, 1989; revised October 20, 1989

The oxidative dehydrogenation of propane was studied on a V–Mg–O catalyst for possible gas-phase reactions initiated by the desorption of reactive intermediates from the catalyst surface. It was found that the conversions of propane at 556 and 570°C in the void volume positioned immediately downstream of the catalyst were higher than those in the same void volume positioned upstream of the catalyst, and much higher than those in the absence of the catalyst. The propane conversion due to postcatalytic reactions increased with the weight of the catalyst wafer, the propane/oxygen partial pressure, and the propane/oxygen ratio. That this conversion was much higher in the presence than in the absence of a catalyst was due to the heats of reaction generated on the catalyst surface and gas-phase reactions of propane initiated by the desorption of free radicals or reactive intermediates from the catalyst surface. It was also established that at 585°C there were few reactions due to the oxidative pyrolysis of methane, ethene, or propene. These results strongly suggested that the overall reaction mechanism consisted of a heterogeneous, a heterogeneous–homogeneous, and a homogeneous reaction pathway.

INTRODUCTION

Radical species have long been proposed as possible intermediates in a number of catalytic hydrocarbon oxidation reactions. Recently, there has been increasing evidence that some of these radical species may desorb into the gas phase to initiate homogeneous reactions (*1*). Latyshev and Popova have reported that in the butene oxidation on a copper oxide catalyst, the gas-phase temperature downstream from the catalyst was higher than the surface reaction temperature, presumably due to a heterogeneous–homogeneous reaction (*2*). Other workers have reported that different reaction products were obtained depending on the postcatalytic volume in butene oxidation on Fe–Sb–O (*3*) and propene oxidation on Bi–Mo–O (*4–6*) under conditions where few reactions occurred in the absence of a catalyst. Direct detection of desorbed radicals by EPR has been achieved using the matrix isolation technique in the oxidative coupling of methane on Li/MgO (*7*) and propene on Bi_2O_3 catalysts (*8*). In these reactions, a C–H bond is first broken to form a methyl or a π-allyl species, respectively. These species can either remain on the surface to react further or desorb into the gas phase as radicals and further react to form the stable products.

It has been reported earlier that V–Mg–O catalysts are selective for the oxidative dehydrogenation of light alkanes, especially propane and butane (*9, 10*). At low conversions, selectivities of 70–80% for dehydrogenation products were obtained. In the case of butane, a selectivity of over 50% was obtained even at high conversions. It was suggested that the reaction proceeds via the formation of an alkyl species. For propane, this involves the breaking of primarily a methylene C–H bond to form an adsorbed propyl radical and a surface OH group. In this aspect, the proposed reaction mechanism is similar to other reaction mechanisms proposed for the oxidative

---

[1] To whom correspondence should be addressed.

0021-9517/90 $3.00

coupling of methane (*7*) and propene (*8, 11*). It became interesting to investigate if the phenomenon of radical desorption also occurred on the V–Mg–O catalysts for the oxidative dehydrogenation of light alkanes. Here we report the results of such an investigation.

The technique used in this study involved adding a postcatalytic volume after the catalyst. If the reaction was entirely heterogeneous, the reaction intermediates would remain adsorbed on the surface and react further to yield the final products before desorption. The presence of a void volume (hereafter, termed postcatalytic volume) after the catalyst bed should not affect the conversion or product selectivity of the reaction. If the reaction involved a heterogeneous–homogeneous pathway, some surface reaction intermediates would desorb into the postcatalytic volume and react further in the gas phase. Consequently, the presence of a large postcatalytic volume would increase the conversion and possibly change the product distribution. Therefore, by determining the conversion and product selectivities in both the presence and the absence of the postcatalytic volume, the importance of the heterogeneous–homogeneous pathway could be evaluated.

EXPERIMENTAL

Catalyst Preparation

MgO was prepared by precipitation from a magnesium nitrate (Aldrich Chemicals, ACS grade) solution with ammonium carbonate (Alfa Products, ACS grade). The precipitate was suction-filtered and washed with doubly distilled water. The pH of the final filtrate was near 7. The solid was then dried at about 80°C overnight, followed by calcination in air at 700°C for 3 h. The BET surface area as measured by N_2 adsorption was 28 m^2/g.

V–Mg–O catalysts were prepared as follows: An appropriate amount of NH_4VO_3 (Johnson Matthey, 99%) was dissolved in hot doubly distilled water. This solution was added in small portions to a crystallization dish containing a predetermined amount of MgO. The excess water from the resultant slurry was evaporated on a stirring hotplate. This step was repeated until all the vanadate solution was added. The slurry was concentrated on the hotplate into a thick paste form. This paste was then dried at about 80°C overnight. The dried solid was calcined in air at 580°C for 6 h. The catalyst used in this study was labeled 19V–Mg–O and its composition as determined by atomic absorption spectroscopy was 19 wt% V_2O_5 and 81 wt% MgO. The BET surface area was 48 m^2/g.

ZnO was prepared by precipitation from a zinc nitrate (Aldrich, ACS grade) solution with sodium carbonate (Alfa Products, ACS grade). The precipitate was suction-filtered and washed with distilled water. The cake was dried in air at about 80°C overnight and then calcined in air at 400°C for 6 h. The BET surface area was 10 m^2/g.

Self-supporting catalyst wafers were made by pressing 0.033 g of the powder with a hydraulic press at 7 MPa pressure. They were used instead of loose powder so that desorbed species could desorb into the postcatalytic volume directly without having to pass through a layer of supporting quartz wool. The diameters of the wafers were 14 mm, and the thicknesses were less than 1 mm. Wafers of different weights were obtained by cutting equal parts from both the top and the bottom of a wafer using a sharp razor blade. Wafers of 0.016, 0.021, and 0.027 g were used.

Experimental Apparatus

A quartz reactor with an inner and an outer diameter of 15.5 and 17 mm, respectively, was used in a horizontal position. The catalyst wafer was positioned upright in a specially designed quartz holder inside the reactor as shown in Fig. 1. A short quartz cylinder (inner and outer diameters were 13 and 14 mm, respectively and a length of 25.4 mm) with four fingers attached to one end of the cylinder was used

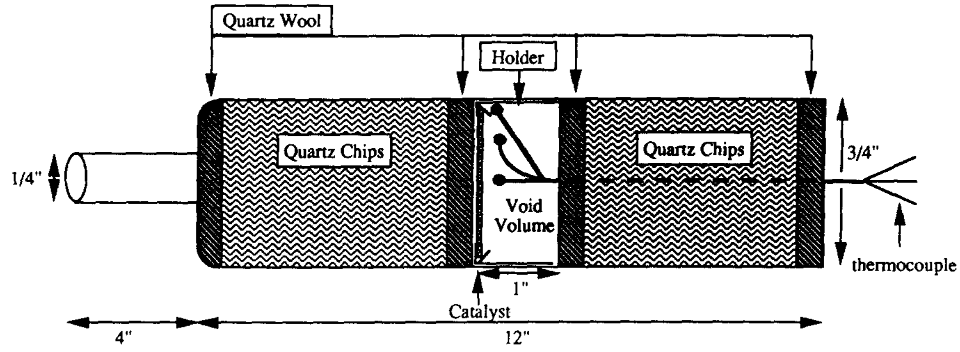

FIG. 1. Schematic diagram of the reactor.

as the holder for the catalyst wafer. On one side of the catalyst wafer the reactor volume was packed with a 3-mm layer of quartz wool followed by quartz chips. An about 2.5-cm length of the reactor on the other side could be left empty as the void volume. Since the reactant feed could be controlled to enter the reactor from either end by a 4-way Carle valve, this void volume could act as either a precatalytic (before the catalyst wafer) or a postcatalytic (after the catalyst wafer) volume. The remainder of the reactor was packed with quartz chips. The same void volume was used without a catalyst wafer to obtain oxidative pyrolysis results.

Quartz chips were found to be very effective radical quenchers. In an empty reactor (volume = 63.2 ± 0.2 ml), a propane conversion of 90% was observed at 570°C using a feed of 4 vol% propane, 8 vol% oxygen, and the balance helium and a total flow rate of 100 ml/min. When the reactor was packed with quartz chips, the propane conversion was reduced to about 1%. Therefore, in all the experiments any unused portion of the reactor volume was packed with quartz chips to minimize unwanted gas-phase reactions.

The temperature outside the reactor was measured by a thermocouple positioned such that the tip touched the outside wall of the reactor at the position of the catalyst wafer. The thermocouple was used as input to the temperature controller. The temperature on the outside of the reactor along the position of the void volume was maintained constant to within ±1.5°C. Unless specified, the temperatures referred to here are the temperature readings on the outside wall of the reactor. The radial and axial temperature profiles in the void volume inside the reactor were determined using chromel–alumel thermocouples. The thermocouple tips were directly exposed to the reaction mixture, and the wires were insulated with MgO packed in a stainless-steel sheath. The radial temperature profile was measured by three thermocouples positioned at the center of the void volume, at the wall of the catalyst holder, and roughly in between these two thermocouples. The axial temperature profile was measured by moving the thermocouples inside the reactor from nearly touching the catalyst wafer to the end of the void volume.

The reaction feed was 4 to 8 vol% propane (Linde, CP grade), 8 to 16 vol% oxygen (Linde, hydrocarbon free grade), and the balance helium (Linde, Zero grade). The flow rate was 100 ml/min unless indicated otherwise, and the furnace temperature was set at 556 and 570°C. The reaction products were analyzed by on-line gas chromatography. Two columns were used in parallel to separate the products: an 8 ft × $\frac{1}{8}$ in. carbosphere column at 40°C to separate oxygen, carbon monoxide, and methane, and a 12 ft × $\frac{1}{4}$ in. tetraglyme coated on Chromosorb P column at 0°C to separate

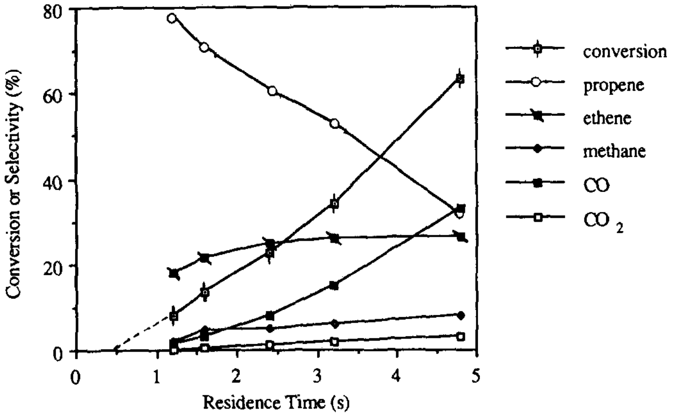

FIG. 2. Product selectivities (C_3 basis) and conversions of oxidative pyrolysis of propane at 570°C as a function of residence time. $C_3H_8/O_2/He = 6/12/82$.

the hydrocarbons. Hydrogen and water were not analyzed.

RESULTS

Oxidative Pyrolysis

The oxidative pyrolysis of propane without catalyst was investigated at reaction temperatures of 556 and 570°C and at residence times up to 2.4 s. Residence times were obtained by dividing the volume of the reaction zone (5.6 ± 0.2 ml) by the volumetric flow rate of the feed measured at reaction temperatures. The actual residence times of the gases in the reaction zone were slightly less, depending on the conversion, since there was an increase in the number of moles of gas because of the oxidative pyrolysis reactions. The residence times were varied by changing the flow rate. Figure 2 shows the product distribution as a function of residence time at 570°C. Below about 45% conversion or 3.5 s residence time, propene and ethene were the major products. The minor products were methane and carbon oxides. No ethane, oxygenates, or C_4 hydrocarbons were detected. The carbon balance in all the reaction runs was within ±3%. As the residence time increased, the selectivity to propene decreased, while the selectivities to the other products increased. A similar trend was also observed at 556°C as shown in Fig. 3.

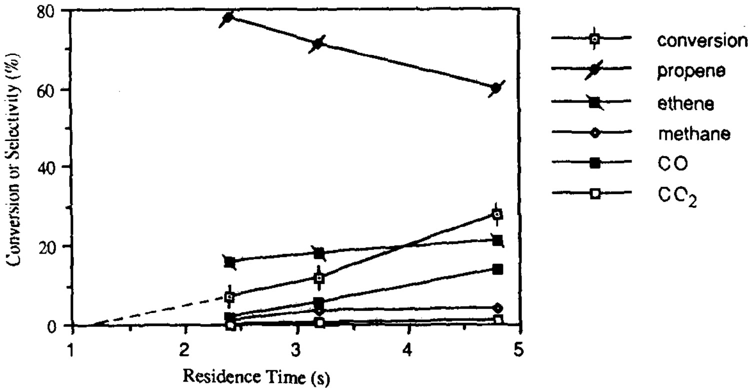

FIG. 3. Product selectivities (C_3 basis) and conversions of oxidative pyrolysis of propane at 556°C as a function of residence time. $C_3H_8/O_2/He = 6/12/82$.

TABLE 1

Oxidative Pyrolysis of Propane in a Void Volume of 5.6 ml

	Temperature					
	556°C			570°C		
Feed ($C_3H_8 : O_2 :$ He)	4 : 8 : 88	6 : 12 : 82	8 : 16 : 76	4 : 8 : 88	6 : 12 : 82	8 : 16 : 76
C_3H_8 conversion (%)	2.8	3.8	8.7	8.1	14.6	23.1
O_2 conversion (%)	1.5	1.8	2.0	2.5	2.7	6.5
Carbon product distribution (% C_3H_8 basis)						
CO	0.5	1.2	2.3	1.2	5.7	5.5
CO_2	2.6	4.0	2.4	0.8	1.5	1.8
CH_4	2.7	3.4	2.8	6.2	6.3	6.5
C_2H_4	13.8	14.2	14.4	19.8	19.0	21.6
C_3H_6	80.4	79.2	78.1	71.9	67.5	64.7

The effect of the partial pressures of propane and oxygen was studied at 556 and 570°C. The propane concentration was increased from 4 to 8 vol% while maintaining the O_2/C_3H_8 ratio at 2. As expected, the conversion increased with the partial pressure of propane and oxygen as shown in Table 1 for reaction temperatures of 556 and 570°C, respectively.

The reaction temperature had a pronounced effect on the reaction kinetics and induction period. As shown in Figs. 2 and 3, the induction time decreased from about 1.2 to 0.4 s as the temperature was increased from 556 to 570°C. The reaction rate increased by a factor of about 3 as the temperature was increased from 556 to 570°C as shown in Table 1. The product distribution was only slightly affected by the temperature. For a given conversion, propene selectivity decreased slightly and ethene selectivity increased slightly as the temperature increased.

Catalytic Activity of V–Mg–O Catalyst

To determine the activity of the catalyst wafer without contribution from gas-phase reactions, the reactor was filled with quartz chips up to the catalyst wafer. In this arrangement, any radicals desorbed from the catalyst into the gas phase would be quenched immediately by the chips. The major products of the reaction were propene, CO, and CO_2. Ethene was the minor product. Ethane was not detected. The carbon balance in all the reaction runs was ±3%. Thus little or no oxygenates were formed. Column 1 in Tables 2 and 3 lists some sample product distributions obtained at 556 and 570°C. At 10% conversion, the

TABLE 2

Conversion and Selectivity of Catalyst Wafer (1), Void Volume (2), Precatalytic Volume + Catalyst Wafer (3), and Catalyst Wafer + Postcatalytic Volume (4), T = 556°C, Weight of V–Mg–O Catalyst Wafer = 0.021 g

	1	2	3	4
Feed composition $C_3H_8 : O_2 :$ He = 6 : 12 : 82 vol%				
C_3H_8 conversion (%)	10.8	3.8	16.7	22.5
O_2 conversion (%)	10.9	1.3	14.9	13.6
Carbon product sel. (%)				
CO	14.4	0.2	14.9	11.0
CO_2	28.1	4.0	20.8	13.4
CH_4	0.5	3.4	2.6	2.9
C_2H_4	1.4	13.2	8.9	13.1
C_3H_6	55.6	79.2	52.8	59.6
Feed composition $C_3H_8 : O_2 :$ He = 8 : 16 : 76 vol%				
C_3H_8 conversion (%)	11.3	8.7	24.9	32.8
O_2 conversion (%)	10.2	2.0	23.0	19.1
Carbon product sel. (%)				
CO	17.6	2.3	13.6	12.2
CO_2	30.2	2.4	20.2	11.9
CH_4	0.8	2.8	1.5	2.9
C_2H_4	1.3	14.4	11.3	14.6
C_3H_6	50.1	78.1	53.4	58.4

TABLE 3

Conversion and Selectivity of Catalyst Wafer (1), Void Volume (2), Precatalytic Volume + Catalyst Wafer (3), and Catalyst Wafer + Postcatalytic Volume (4), $T = 570°C$, Weight of V–Mg–O Catalyst Wafer = 0.021 g

	1	2	3	4
Feed composition $C_3H_8 : O_2 : He = 6 : 12 : 82$ vol%				
C_3H_8 conversion (%)	15.2	14.6	33.2	46.2
O_2 conversion (%)	15.7	2.7	23.7	27.1
Carbon product sel. (%)				
CO	15.3	5.7	18.0	16.3
CO_2	28.6	1.5	20.8	9.8
CH_4	1.7	5.3	5.1	6.2
C_2H_4	3.8	19.0	15.2	22.8
C_3H_6	50.6	68.5	40.9	44.9
Feed composition $C_3H_8 : O_2 : He = 8 : 16 : 76$ vol%				
C_3H_8 conversion (%)	17.0	23.1	42.3	69.3
O_2 conversion (%)	12.0	6.5	41.9	38.7
Carbon product sel. (%)				
CO	15.4	5.5	20.7	21.4
CO_2	26.2	1.8	17.1	8.5
CH_4	1.3	3.5	4.5	5.4
C_2H_4	4.5	18.6	17.2	27.4
C_3H_6	52.6	70.7	40.5	37.3

selectivity for propene using a wafer was about 10% lower than that using a powder catalyst (*10, 12*). The conversion of propane increased as the partial pressure of propane was increased from 4 to 8 vol% while the C_3H_8/O_2 ratio was maintained constant at 1/2. Assuming that the rate of reaction was independent of the oxygen partial pressure as reported earlier (*10*), the reaction order in propane partial pressure was calculated to be 0.6, which is consistent with the results reported earlier (*10*).

Precatalytic Volume and V–Mg–O Catalyst

The conversions and the product selectivities in the precatalytic volume arrangement were determined at 556 and 570°C using a feed that contained 4 to 8% propane and a fixed ratio of oxygen to propane of 2. Column 3 in Tables 2 and 3 shows the typical results obtained at 556 and 570°C, respectively. Also shown in these tables are the activities of the catalyst wafer (column 1) and of the void volume (column 2), which were determined individually.

V–Mg–O Catalyst and Postcatalytic Volume

The conversions and product selectivities for the postcatalytic volume arrangement were determined. Column 4 of Tables 2 and 3 shows the typical results obtained at 556 and 570°C, respectively. The major products were C_3H_6, C_2H_4, CH_4, CO, and CO_2. Ethane was not found. The carbon balances in all the reaction runs were ±3%. Thus little or no oxygenates were formed. At 556°C or higher, the propane conversions in this arrangement (X_{post}) were

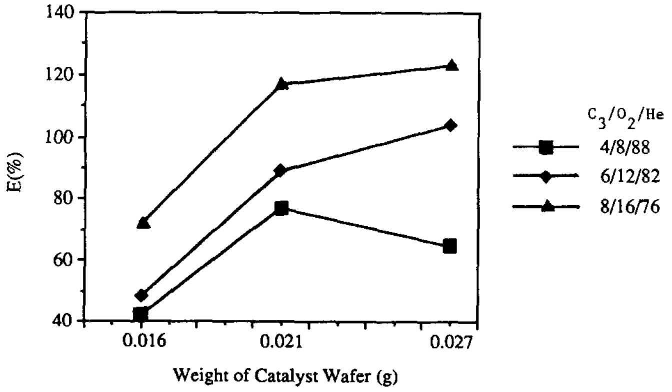

FIG. 4. Extent of enhancement (E) as a function of the weight of catalyst wafer at 570°C.

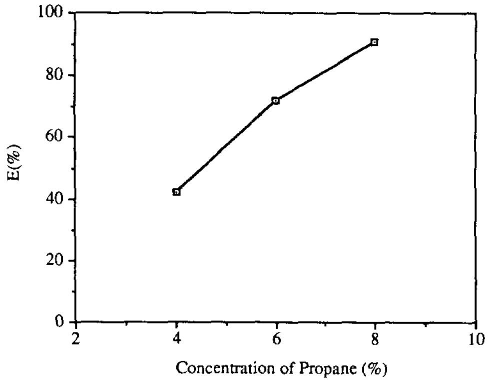

FIG. 5. Extent of enhancement as a function of propane concentration at 570°C. Oxygen concentration = 8%, 0.021 g catalyst.

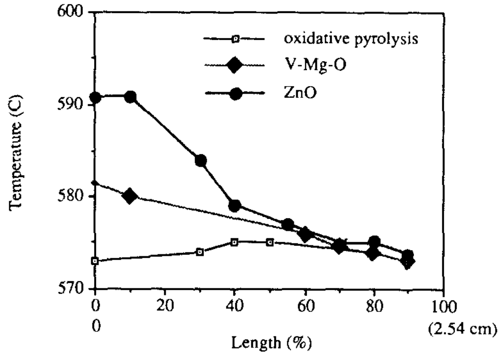

FIG. 6. Axial temperature profile measured from the position of the catalyst wafer in the void volume in the precatalytic arrangement. 0.021 g of V–Mg–O catalyst, 570°C, $C_3H_8/O_2/He$ = 6/12/82.

higher than the precatalytic volume arrangement (X_{pre}) under otherwise identical conditions.

The extent of enhancement in the conversion of propane, E, can be defined as

$$E\,(\%) = \frac{X_{\mathrm{post}} - X_{\mathrm{pre}}}{X_{\mathrm{vol}}} \times 100,$$

where X_{vol} is the propane conversion in the void volume which was determined independently (column 2 in Tables 2 and 3). It was found that E increased with the weight of the catalyst wafer, the partial pressure of propane and oxygen, and the propane/oxygen ratio as shown in Figs. 4 and 5. No enhancement was observed at 540°C.

Temperature Measurements

The axial temperature profile at the central position in the void volume was measured in both the precatalytic and the postcatalytic volume arrangements using a feed of 6% propane, 12% oxygen, and the balance helium, a 0.021 g catalyst wafer, and a reaction temperature of 570°C. The results are shown in Figs. 6 and 7. In the absence of the catalyst wafer, a temperature rise of about 4°C was detected in the void volume due to the oxidative pyrolysis reactions. For the ZnO catalyst in the precatalytic volume arrangement, a temperature rise of about 20°C was observed near the wafer, which decreased gradually to about 4°C away from the wafer, which was the temperature rise due to the oxidative pyrolysis reactions. The temperature profile was similar in the postcatalytic volume arrangement, except that the magnitude of the temperature rise was slightly higher. For the V–Mg–O catalyst, the rise was about 11°C near the wafer and decreased gradually to about 4°C away from the wafer. Again, the magnitude of the rise was slightly larger in the postcatalytic than the precatalytic volume arrangement.

Figure 8 shows the radial temperature profile in the postcatalytic arrangement us-

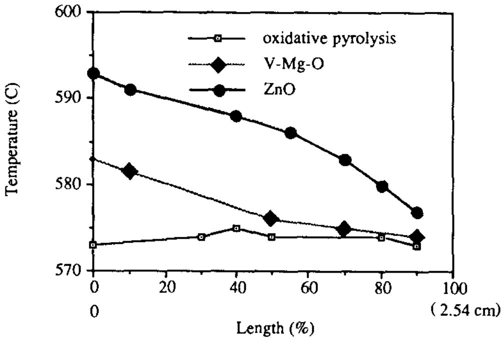

FIG. 7. Axial temperature profile measured from the position of the catalyst wafer in the void volume in the postcatalytic arrangement. 0.021 g of V–Mg–O catalyst, 570°C, $C_3H_8/O_2/He$ = 6/12/82.

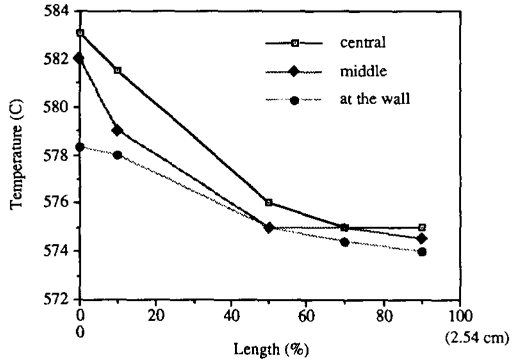

FIG. 8. Radial temperature profile measured from the center to the wall of the reactor in the postcatalytic volume arrangement. Same conditions as those in Fig. 7.

ing the V–Mg–O catalyst. The temperature in the central position was always the highest, whereas that near the holder wall was the lowest. The difference between the two positions near the catalyst wafer was 5°C, which decreased to only 1°C at the end of the void volume. The temperature profile was similar in the precatalytic volume arrangement, except that the magnitude of the difference near the catalyst wafer was 4°C.

ZnO Catalyst

The catalytic activity of ZnO catalyst was determined at 570°C using a feed of $C_3H_8/O_2/He$ = 6/12/82. The propane conversion and the product distribution are shown in column 1 of Table 4. The selectivity to carbon oxides was about 90%. Other minor products were propene and ethene. Also shown in Table 4 are the results in which the ZnO catalyst wafer was used in the precatalytic (column 3) and postcatalytic (column 4) volume arrangements. Combustion was still the primary reaction in these arrangements, but the selectivities for ethene and propene were higher than those in the absence of the void volume. It should be noted that the conversion in the precatalytic volume and the postcatalytic volume arrangements were similar; that is, there was no enhancement in conversion.

MgO Catalyst

The conversion and product distribution for a 0.05-g MgO catalyst wafer were determined at 570°C with a feed of $C_3H_8/O_2/He$ = 6/12/82. The results are shown in Table 5. In the absence of the void volume, the selectivity to carbon oxides was 61%, while the selectivity to propene was 30%. Other minor products were ethene and methane. Within experimental error, the conversions in both precatalytic and postcatalytic volume arrangements were similar (Table 5). Thus like ZnO, MgO did not cause any enhancement in the conversion.

TABLE 4

Conversion and Selectivity of Catalyst Wafer (1), Void Volume (2), Precatalytic Volume + Catalyst Wafer (3), and Catalyst Wafer + Postcatalytic Volume (4), $T = 570°C$, feed ($C_3H_8:O_2:He = 6:12:82$ vol%), Weight of ZnO Catalyst Wafer = 0.0984 g

	1	2	3	4
C_3H_8 conversion (%)	10.2	14.6	32.6	32.1
O_2 conversion (%)	14.6	2.7	55.0	33.2
Carbon product sel. (%)				
CO	39.7	5.7	14.5	10.1
CO_2	49.9	1.5	52.2	37.2
CH_4	0	5.3	1.0	3.7
C_2H_4	6.5	19.0	18.7	18.2
C_3H_6	3.9	68.5	13.6	30.7

TABLE 5

Conversion and Selectivity of Catalyst Wafer (1), Void Volume (2), Precatalytic Volume + Catalyst Wafer (3), and Catalyst Wafer + Postcatalytic Volume (4), $T = 570°C$, feed ($C_3H_8:O_2:He = 6:12:82$ vol%), Weight of MgO Catalyst Wafer = 0.050 g

	1	2	3	4
C_3H_8 conversion (%)	12.0	14.6	30.8	31.6
O_2 conversion (%)	14.8	2.7	28.7	28.7
Carbon product sel. (%)				
CO	8.5	5.7	12.8	6.8
CO_2	52.2	1.5	24.6	20.9
CH_4	2.6	5.3	4.9	5.9
C_2H_4	6.3	19.0	17.5	22.8
C_3H_6	30.4	68.5	40.2	43.6

DISCUSSION

Oxidative Pyrolysis

The results of the oxidative pyrolysis of propane are shown in Figs. 2 and 3. The conversion curves in these figures show the presence of an induction period, which is much shorter at the higher temperature. The presence of an induction period is often found in chain reactions, which has been proposed for this reaction (*13*). In the proposed mechanism, the initiation steps are (*13*)

$$C_3H_8 \rightarrow \cdot C_2H_5 + \cdot CH_3 \qquad (1)$$

$$\cdot CH_3 + C_3H_8 \rightarrow CH_4 + \cdot C_3H_7 \qquad (2)$$

$$\cdot C_2H_5 + C_3H_8 \rightarrow C_2H_6 + \cdot C_3H_7 \qquad (3)$$

and the major propagation steps are

$$\cdot C_3H_7 + O_2 \rightarrow C_3H_6 + \cdot HO_2 \qquad (4)$$

$$\cdot C_2H_5 + O_2 \rightarrow C_2H_4 + \cdot HO_2 \qquad (5)$$

$$\cdot C_3H_7 \rightarrow C_2H_4 + \cdot CH_3 \qquad (6)$$

$$\cdot HO_2 + \cdot HO_2 \rightarrow H_2O_2 + O_2 \qquad (7)$$

$$\cdot HO_2 + C_3H_8 \rightarrow H_2O_2 + \cdot C_3H_7 \qquad (8)$$

$$C_3H_8 + O_2 \rightarrow \cdot HO_2 + \cdot C_3H_7 \qquad (9)$$

$$H_2O_2 \rightarrow 2\cdot OH \qquad (10)$$

$$C_3H_8 + \cdot OH \rightarrow \cdot C_3H_7 + H_2O \qquad (11)$$

The above mechanism explains the product distribution obtained in this study. It has been observed that the major products are propene and ethene at low conversions. The selectivity to alkenes decreases as conversion increases, but for the same conversion, it is higher than the values obtained in reactions over $ZnWO_4$ (*14*) or over V–Mg–O catalysts (*10*). It is also higher than pyrolysis in the absence of oxygen (*13*). The product distributions obtained here are similar to those reported by Layokun (*13*) and Taylor and Kulich (*15*).

Catalytic Activity of V–Mg–O Catalyst

The product selectivities and the reaction orders using a wafer were similar to those obtained using a powder catalyst. The slightly lower selectivities for propene could be due to consecutive reactions of propene formed inside the wafer.

For the catalyst wafer made with 0.021 g of powder, an "effectiveness factor" was determined to be about 80–85% from the ratio of the catalytic activity of the wafer and the activity of the catalyst powder having the same weight.

ZnO Catalyst

As shown in Table 4, ZnO is not a selective oxidative dehydrogenation catalyst. The major products are CO and CO_2. This is consistent with the results reported by Takami and co-worker (*14*). In the precatalytic and postcatalytic volume arrangements, the propane conversions were 32.6 and 32.1%, respectively, 7.8 and 7.3% higher than the conversions expected on the basis of the independent measurements of the wafer and the void volume. If the wafer and the volume acted independently, the total conversion should be 24.8%. The increases are attributed to the effect due to the heat of reaction, as is discussed later.

MgO Catalyst

As shown in Table 5, MgO is not a selective oxidative dehydrogenation catalyst. The major product is CO_2. Propene is produced with a higher selectivity than on ZnO but is much lower than on V–Mg–O. In the precatalytic and postcatalytic volume arrangements, the propane conversions were 30.8 and 31.6%, respectively. These values are 4.2 and 5.0% higher than the conversions expected on the basis of independent measurements of the wafer and the void volume. If the wafer and the volume acted independently, the total conversion should be 26.6%. The increases are also attributed to the effect due to the heat of reaction as discussed in the next section. This is consistent with the results of Lunsford and coworkers, who have shown that MgO catalysts are relatively inactive as alkyl radical generators (*16*).

TABLE 6

Conversions of Catalyst Wafer (1), Void Volume (2), Precatalytic Volume + Catalyst Wafer (3), and Catalyst Wafer + Postcatalytic Volume (4) and Extent of Enhancement (5) for 0.021 g V–Mg–O Catalyst Wafer

Feed ($C_3H_8:O_2:He$)	T (°C)	1 X_{cat} (%)	2 X_{vol} (%)	3 X_{pre} (%)	4 X_{post} (%)	5 E (%)
4:8:88	570	11.0	8.1	22.4	28.6	77
6:12:82	570	15.2	14.6	33.2	46.2	89
8:16:76	570	17.0	23.1	42.3	69.3	117
4:8:88	556	7.7	2.8	12.3	15.6	118
6:12:82	556	10.8	3.8	16.7	21.5	152
8:16:76	556	11.3	8.7	24.9	32.8	91
4:8:88	540			14.0	13.6	0

Precatalytic Volume—V–Mg–O Catalyst Arrangement

In the precatalytic volume arrangement, the reactant feed first enters the void volume where oxidative pyrolysis occurs. The reaction mixture then passes over the catalyst wafer. If the void volume and the catalyst wafer acted independently, the total conversion should be the sum of the conversions due to the void volume and due to the catalyst wafer. However, as shown in Table 6, the observed total conversions are consistently higher than the sum of the conversions of the catalyst wafer and the volume. This behavior is also observed using ZnO or MgO as the catalyst (Tables 4 and 5). Since the catalytic properties of these oxides are quite different, e.g., the product distributions are different, it is likely that the above observation is due to the heat of reaction and not desorption of reactive intermediates that would induce reactions in the gas phase. This is substantiated by the following example.

In the experiment using $C_3H_8/O_2/H_2$ = 6/12/82 at 570°C and 0.021 g of V–Mg–O, the temperature in the void volume was found to be higher than the outside furnace temperature as is shown in Fig. 6. The temperature was as high as 582°C near the catalyst wafer and decreased gradually away from it to about 574°C. The conversion of propane in this experiment was 33.2%, which was 3.4% higher than the expected conversion of 29.8% if the wafer and the void volume acted independently at 570°C. At 570°C, the conversion in the void volume without the catalyst was 14.6%, and it was 19% if the temperature was 585°C. Thus a void volume hotter by 15°C would result in an increase in conversion of 4.4%. Since the void volume in the precatalytic volume arrangement was not uniformly hot, the increase in the total conversion would be less than 4.4%, as was observed.

One would expect the thermal effect to be much more significant with the ZnO catalyst than with the V–Mg–O catalyst, since the major products of the reaction on ZnO are carbon oxides, and the combustion reaction has a higher rate of heat release into the gas phase than dehydrogenation reactions. Indeed, the temperature rise near the ZnO catalyst wafer was 21°C (Fig. 6), much higher than that detected when V–Mg–O was used, and the total conversion was 32.6%, which was 8% higher than the sum of the independent conversions of the catalyst and the volume of 24.6%.

In view of these results, it is concluded that the total conversion in the precatalytic volume arrangement is due to the contribution of the conversion on the catalyst and the conversion in the void volume at an elevated temperature. There is no need to as-

TABLE 7

Propane Conversions and Product Distributions in the Separate Reactor Arrangement[a] (0.021 g Catalyst, $C_3H_8/O_2/He$ = 6/12/82)

	Catalyst[b]	Cat + Vol[c]	Cat + Vol[c]
Void volume temperature (°C)		570	585
C_3H_8 conversion (%)	15.4	27.9	33.9
O_2 conversion (%)	13.6	18.1	29.6
Carbon product distribution (% C_3H_8 basis)			
CO	21.1	11.1	17.9
CO_2	27.4	12.3	17.7
CH_4	0	4.9	2.5
C_2H_4	3.3	14.1	14.1
C_3H_6	48.2	58.8	45.5

[a] Catalyst wafer in the first reactor, void volume in the second reactor.
[b] No void volume in the second reactor.
[c] Catalyst wafer at 570°C.

sume any desorption of radicals from the catalyst that could induce reactions in the void volume.

Postcatalytic Volume Arrangement with V–Mg–O Catalyst

In the postcatalytic arrangement, the feed first reacts on the catalyst wafer before it enters the void volume, where oxidative pyrolysis occurs. In this arrangement, if the catalyst wafer and the postcatalytic volume behave independently, the total conversion should be the sum of the conversion due to the void volume and that of the catalyst wafer. However, as shown in Table 6, the observed conversions are consistently higher than the sum of the conversions of the void volume and the catalyst wafer. They are also higher than X_{pre}. There are three possible explanations for the high value of X_{post}. It could be a result of heats of reaction generated on the catalyst surface, reactions of alkenes or other products with propane, or reactions of propane initiated by the desorption of free radicals or other highly reactive intermediates into the gas phase.

The effect of the heat of reaction was examined as follows. In the experiment using $C_3H_8/O_2/He$ = 6/12/82 at 570°C and 0.021 g of V–Mg–O catalyst, the temperature profile inside the reactor void volume was measured. The temperature in the void volume was found to be higher than the outside furnace temperature as shown in Fig. 7. If the effect is entirely due to this increase in temperature in the void volume, the same conversion should be obtained if the catalyst wafer and the void volume are separated so long as the temperature of the void volume is reproduced. To accomplish this, a series of experiments were run using two reactors in series. The first reactor contained only the catalyst wafer at 570°C and no void volume. The second reactor contained only the void volume and its temperature was independently adjusted. In these experiments, the products from the catalyst wafer obtained at 570°C in the first reactor were first quenched to room temperature and then sent to the second reactor. The second reactor was then heated to an outside furnace temperature of 570 or 585°C. The results of these experiments are shown in Table 7. At 570°C, the total propane conversion was 27.9%. This conversion was comparable to the sum of the conversions of the catalyst wafer and the void volume shown in Table 6. At 585°C the total propane conversion was 33.9%. This 6% increase in propane conversion represents the result of heating of the void volume due to the heat of reaction released from the catalyst. It also represents the maximum increase in propane conversion caused by the thermal effect, since the high temperature is maintained throughout the second reactor in this control experiment and does not fall off at one end as in Fig. 7.

The results of these control experiments using separate reactors also exclude the second possible explanation that the high X_{post} values are due to reactions of alkenes or other products with propane. No substantial reactions due to the oxidative pyrolysis of methane, ethene, or propene occurred at 585°C. Temperatures above 625°C are required for methane oxidation (*7*), and above 630°C for propene (*17*). On the other hand, thermal effect can account for the high X_{post} values for ZnO and MgO. On these two catalysts, the total conversions in the precatalytic volume and the postcatalytic volume arrangements are similar. This is consistent with the similar temperature profiles in both arrangements for ZnO as shown in Figs. 6 and 7. For the thermal effect, the direction of flow of reactants should not be important, which is what has been observed.

It is likely that the enhancement of the propane conversion in the postcatalytic volume arrangement is due to gas-phase reactions induced by the desorption of reactive intermediates from the V–Mg–O catalyst. The extent of enhancement (E) as defined represents the percentage increase in the rate of propagation excluding that due to thermal effects in the postcatalytic volume above the rate of oxidative pyrolysis in the absence of the catalyst. It is important to emphasize that the thermal effect has been corrected for in the calculation of E by taking the difference between the conversions in the precatalytic and the postcatalytic volume arrangements. If E is zero, then the rate of propagation in the postcatalytic volume is identical to the rate of propagation in the void volume at the same temperature in the absence of a catalyst, which would indicate that there are no radicals desorbed from the catalyst surface into the gas phase. If E is greater than zero, it would indicate that some radicals are generated by the catalyst and desorbed into the gas phase to enhance the propagation reaction in the postcatalytic volume.

If radical desorption occurs in the postcatalytic volume arrangement, the extent of enhancement should increase with the amount of radicals desorbed, which depends on the weight of the catalyst wafer, and the propane/oxygen partial pressure and temperature. Indeed, E increases generally with increasing weight of the catalyst wafer as shown in Fig. 4. Also, E increases when the C_3H_8/O_2 feed is increased from 4/8 to 8/16 as well as when the partial pressure of propane is increased (Fig. 5).

From the activities and product distributions obtained in the postcatalytic volume arrangement (column 4 of Tables 2 and 3) and the corresponding data for the catalyst wafer, the selectivity of product a formed in the postcatalytic volume (S_{ap}) can be calculated:

$$S_{\mathrm{ap}} = \frac{(S_{\mathrm{a}}X)_{\mathrm{post}} - (S_{\mathrm{a}}X)_{\mathrm{cat}}}{X_{\mathrm{post}} - X_{\mathrm{cat}}}.$$

These values are shown in Table 8. When these product selectivities are compared with those obtained in the oxidative pyrolysis at the same conversions, it is found that at 556°C, the product distributions are very similar, as shown in Table 8. At 570°C, the selectivities to CO, CO_2, and CH_4 are similar. However, the selectivities to ethene are higher, while those to propene are lower than those of oxidative pyrolysis. These differences can be attributed to the higher reaction temperature, 582°C, in the postcatalytic volume due to the reactions on the catalyst wafer than the reaction temperature in oxidative pyrolysis which is close to 574°C. It has been reported that in oxidative pyrolysis the selectivity to ethene increases while that to propene decreases as the reaction temperature is increased (*13*).

Reaction Mechanism and Nature of Desorbed Radicals

Previously, we proposed that the breaking of a methylene C–H bond in propane to form an adsorbed propyl species and a surface OH group is the first step of the reaction (*10, 11*). The adsorbed propyl species can react further by rapid breaking of a second C–H bond at the neighboring carbon, resulting in the formation of propene which then desorbs from the surface. In addition to the formation of propene, propyl species also form carbon oxides on the surface. This mechanism applies to reactions at temperatures below 556°C. However, as the results in this study show, above this temperature, a heterogeneous–homogeneous reaction pathway must be considered in addition to the surface reactions.

The fact that the product distributions obtained in the postcatalytic volume are similar to those obtained in the oxidative pyrolysis reactions suggests that the reactions in the postcatalytic volume proceed according to the chain reaction mechanism. It also indicates that the free radicals desorbed from the surface are similar to those generated in the oxidative pyrolysis reactions. These reactive species include alkyl and ·OH which are known to be effective radical propagators at high temperatures. From the data presented, however, it is impossible to identify which radicals are desorbed. We are attempting to model the reactions in the postcatalytic volume with the hope of answering this question. Results of the modeling study will be reported later.

In conclusion, we have shown that above 556°C reactive intermediates are desorbed from the V–Mg–O catalyst during oxidative dehydrogenation of propane. These desorbed intermediates result in further reaction of propane in the gas phase. Thus the overall reaction mechanism of propane oxidation on V–Mg–O catalyst consists of heterogeneous, heterogeneous–homogeneous, and homogeneous reaction pathways at reaction temperatures above 556°C.

TABLE 8

Comparison of Product Distributions due to Reactions in the Postcatalytic Volume in the Presence of V–Mg–O Catalyst and the Oxidative Pyrolysis (0.021 g Catalyst)

	Postcat. volume	Oxidative pyrolysis	Postcat. volume	Oxidative pyrolysis
Reaction temperature: 556°C				
$C_3H_8/O_2/He$	6/12/82	6/12/82	8/16/76	8/16/76
C_3H_8 conv. (%)	17.8	17.8	21.5	21.5
Carbon product distribution (% C_3H_8 basis)				
CO	7.9	10.0	9.3	12.0
CO_2	0	0	2.3	0
CH_4	5.1	4.0	4.0	3.0
C_2H_4	23.8	19.0	21.6	21.0
C_3H_6	63.2	67.0	62.8	64.0
Reaction temperature: 570°C				
$C_3H_8/O_2/He$	6/12/82	6/12/82	8/16/76	8/16/76
C_3H_8 conv. (%)	31.0	31.0	54.3	54.3
Carbon product selectivity (%)				
CO	16.0	15.5	23.4	23.0
CO_2	0.1	1.0	2.5	2.0
CH_4	8.5	5.0	6.8	6.0
C_2H_4	33.4	25.5	35.2	26.5
C_3H_6	42.0	53.0	32.1	42.5

ACKNOWLEDGMENTS

Support of this work by the U.S. Department of Energy, Basic Energy Sciences Division, and the Mobil Foundation is gratefully acknowledged.

REFERENCES

1. Driscoll, J. D., Campbell, K. D., and Lunsford, J. H., *in* "Advances in Catalysis" (D. D. Eley, H. Pines, and P. B. Weisz, Eds.), Vol. 35, p. 139. Academic Press, San Diego, 1987.
2. Latyshev, J. D., and Popova, N. I., *Kinet. Catal.* **8,** 59 (1967).
3. Shchukin, V., and Ven'yaminov, S. A., *Kinet. Catal.* **11,** 1193 (1970).
4. Daniel, C., and Keulks, G. W., *J. Catal.* **24,** 529 (1972).
5. Daniel, C., Monnier, J. R., and Keulks, G. W., *J. Catal.* **31,** 360 (1973).
6. McCain, C. C., and Godin, G. W., *Nature (London)* **202,** 692 (1964).
7. Driscoll, D. J., Martir, W., Wang, J. X., and Lunsford, J. H., *J. Amer. Chem. Soc.* **107,** 58 (1985).
8. Martir, W., and Lunsford, J. H., *J. Amer. Chem. Soc.* **103,** 3728 (1981).
9. Chaar, M. A., Patel, D. K., Kung, M. C., and Kung, H. H., *J. Catal.* **105,** 483 (1987).
10. Chaar, M. A., Patel, D., and Kung, H. H., *J. Catal.* **109,** 463 (1988).

11. Swift, H. E., Bozik, J. E., and Ondrey, J. A., *J. Catal.* **21,** 212 (1971).

12. Nguyen, K., Ph.D. thesis, Northwestern University (1989).

13. Layokun, S. K., *Ind. Eng. Chem. Process Des. Dev.* **18**(2), 241 (1979).

14. Takami, K., and Imai, H., Report of the Research Laboratory of Engineering Materials, Tokyo Institute of Technology, **6,** 119 (1981).

15. Taylor, J. E., and Kulich, D. M., *ACS Symp. Ser.* **32,** 72 (1976).

16. Martir, W., Ph.D. Dissertation, Texas A & M University (1981).

17. Owen, O., and Kung, H., unpublished results.